*Anal. Chem.* **1996,** *68,* 2905−2912

# Fiber-Optic Evanescent Wave Biosensor for the Detection of Oligonucleotides

Andreas P. Abel, Michael G. Weller,† Gert L. Duveneck, Markus Ehrat,* and H. Michael Widmer

*Corporate Analytical Research, Ciba-Geigy Ltd., CH-4002 Basel, Switzerland*

**An automated optical biosensor system based on fluorescence excitation and detection in the evanescent field of a quartz fiber was used to detect 16-mer oligonucleotides in DNA hybridization assays. A biotinylated capture probe was immobilized on the fiber surface via avidin or streptavidin. The hybridization with fluorescein-labeled complementary strands was monitored in real time by fluorescence detection. The double strands formed by hybridization could be dissociated by chemical or thermal regeneration, allowing one to perform hundreds of assay cycles with the same fiber. The signal loss during long-time measurements, i.e., consecutive hybridization assays, can be described by a single-exponential function. Over more than 200 cycles, the net signal decreased by 50% with a signal variation of 2.4% after correction for this signal loss. By binding the capture probe with the 5′-end to the optical fiber surface, and by using a 50% (w/w) aqueous urea solution for chemical regeneration, the duration of an assay cycle could be reduced to 3 min. By applying longer assay cycles, the detection limit for the hybridization with a complementary fluorescein-labeled oligonucleotide was $2.0 \times 10^{-13}$ M (24 fmol). To detect an unlabeled complementary 16-mer oligonucleotide, competitive hybridization assays were performed, resulting in a detection limit of $1.1 \times 10^{-9}$ M (132 pmol). Poly(acrylic acid) 5100 sodium salt and Tween 20 were used in the hybridization buffer to prevent nonspecific binding caused by ionic or hydrophobic interaction. The amount of nonspecific binding of noncomplementary oligonucleotides was in the range of 1−2%, compared with the specific binding in the different hybridization assays.**

The detection of small variations in the sequence of nucleic acids becomes more and more important, e.g., for the detection of point mutations for the diagnosis of genetic diseases. The capability of DNA and RNA fragments to recognize and bind selectively to complementary arranged nucleotides at other nucleic acids forms an ideal basis for in vitro diagnostic tests. Thus, hybridization methods with nucleic acids as biological recognition elements are a promising supplement to immunoassays: the specificity of nucleic acids for the target analyte can be controlled more easily than that of other biological recognition elements.[1] Hybridization methods can be applied, for example, in human[2] and veterinary[3] medicine, for food quality control,[4] in environmental protection,[5] and in forensic science.[6]

Hybridization methods used today, such as microtiter plates or gel-based methods, are usually quite slow, requiring hours to days to produce reliable results.[7] Biosensors offer a promising alternative for much faster hybridization assays. Biosensors, which are presently being developed for the detection of DNA, are mostly based on surface acoustic wave,[8,9] electrochemical,[10,11] and optical transducers.[12,13] First biosensor systems based on surface plasmon resonance,[14] resonant mirror,[15] grating couplers,[16] and electrochemiluminescence[17] are already commercially available.

We were using a fiber-optic sensor,[18] based on fluorescence excitation and detection in the evanescent field, to detect 16-mer oligonucleotides as a model system. To perform DNA hybridization assays, a capture probe was immobilized on the fiber surface, and the hybridization with fluorescein-labeled complementary strands was monitored by fluorescence detection.

The principle of the evanescent field sensing enables the detection of fluorophores exclusively in the close proximity of the optical fiber.[19] The maximum penetration depth of the evanescent field into the surrounding medium is of the order of some hundred nanometers, allowing detection of the affinity partners which are bound to immobilized recognition elements. Fluorophores outside

† Current address: Institute of Hydrochemistry, Technical University of Munich, D-81377 Munich, Germany.

(1) Deshpande, S. S.; Sharma B. P. In *Diagnostics in the year 2000*; Singh, P., Sharma B. P., Tyle, P., Eds.; Van Nostrand Reinhold: New York, 1993; pp 459−525.
(2) MacPherson, J. M.; Gajadhar, A. A. *Mol. Cell. Probes* **1993**, *7*, 97−103.
(3) Katz, J. B.; Gustafson, G. A.; Alstad, A. D.; Adler, K. A.; Moser, K. M. *Am. J. Vet. Res.* **1993**, *54*, 2021−2026.
(4) Carnegie, P. R. *Australas. Biotechnol.* **1994**, *4 (3)*, 146−149.
(5) Mathe, J.; Eisenmann, C.; Seitz, A. In *DNA fingerprinting: state of the science*; Pena, S. D. J., Chakraborty, R., Epplen, J. T., Jeffreys, A. J., Eds.; Birkhäuser: Basel, 1993; Vol. 67, pp 387−393.
(6) Southern, E. M. *Adv. Forensic Haemogenet.* **1994**, *5*, 103−108.
(7) *DNA probes*; Keller, G. H., Manak, M. M., Eds; Stockton Press: New York, 1993.
(8) Okahata, Y.; Matsunobu, Y.; Ijiro, K.; Mukae, M.; Murakami, A.; Makino, K. *J. Am. Chem. Soc.* **1992**, *114*, 8299−8300.
(9) Su, H.; Yang, M.; Kallury, K. M. R.; Thompson, M.; Roach, A. *Anal. Chem.* **1994**, *66*, 769−777.
(10) Hashimoto, K.; Ito, K.; Ishimori, Y. *Anal. Chem.* **1994**, *66*, 3830−3833.
(11) Millan, K. M.; Saraullo, A.; Mikkelsen, S. R. *Anal. Chem.* **1994**, *66*, 2943−2948.
(12) Piunno, P. A. E.; Krull, U. J.; Hudson, R. H. E.; Damha, M. J.; Cohen, H. *Anal. Chem.* **1995**, *67*, 2635−2643
(13) Pandey, P. C.; Weetall, H. H. *Anal. Chem.* **1995**, *67*, 787−792
(14) Nilsson, P.; Persson, B.; Uhlen, M.; Nygren, P.-A. *Anal. Biochem.* **1995**, *224*, 400−408.
(15) Yeung, D.; Gill, A.; Maule, C. H.; Davies, R. J. *Trends Anal. Chem.* **1995**, *14*, 49−56.
(16) Tiefenthaler, K. *Biosens. Bioelectron.* **1993**, *8* (7/8), xxxv−xxxvii.
(17) DiCesare, J.; Grossman, B.; Katz, E.; Picozza, R.; Ragusa, R.; Woudenberg, T. *BioTechniques* **1993**, *15*, 152−157.
(18) Duveneck, G.; Ehrat, M.; Widmer, H. M. In *Chemical and Medical Sensors*; Wolfbeis, O. S., Ed.; SPIE Proceedings Series 1510; SPIE: Bellingham, WA, , 1991; pp 138−145.
(19) Sutherland, R. M.; Dähne, C.; Place, J. F.; Ringrose A. R. *J. Immunol. Methods* **1984**, *74*, 253−265.

S0003-2700(96)00071-6 CCC: $12.00 

of the evanescent field do not contribute to the emission signal. This allows real-time monitoring of the association and dissociation of analytes during the measurement.[20]

In the future nonisotopic labels,[21,22] such as luminescent markers, have a good chance to replace radiolabels by providing the same or even superior sensitivity but with a reduced disposal problem and better shelf life. Additionally, the handling of nonisotopic labels is considerably safer and therefore does not require specially equipped and certified laboratories. A series of nonisotopic labels, which can be coupled to biomolecules, is already commercially available.[23]

Oligonucleotides are particularly well suited as biological recognition elements. They can be synthesized in a very short time and are available as single-stranded molecules. Every desired base sequence can be chosen for synthesis, making gene probe based tests widely applicable to any complementary sequence of interest.[24] Once double strands (hybrids) are formed, they can be dissociated by heating or chemical treatment. The regeneration of the sensor surface forms the basis of reusable nucleic acid biosensors.

Reusable biosensors have some advantages compared to sensors that are used for only one measurement. The required working steps and time to obtain a reliable result can be reduced and a calibration curve can be applied for a whole series of measurements. A fully automated fluid and data handling system combined with a regenerable biosensor will allow an increase in the reproducibility and the number of measured samples per time compared to traditional methods.[25]

Piunno et al. recently described a similar fiber optic DNA sensor for fluorometric nucleic acid determination.[12] By using ethidium bromide as a fluorescent DNA stain and covalent attachment of the capture probe ($dT_{20}$) to the sensor surface, they achieved a sensitivity of 86 ng/mL DNA, using an assay cycle time of 45 min. With the sensor system described in our work, a labeled oligonucleotide can be detected to 1.3 pg/mL DNA, using an incubation time of 60 min. This is almost $10^5$ times more sensitive than their system and at least $10^2$ times more sensitive for competitive hybridization.

## MATERIALS AND METHODS

**Materials.** The synthetic oligonucleotides were obtained from Microsynth (Balgach, Switzerland) and PAGE-purified. The affinity purified avidin and streptavidin, the biotin-labeled bovine serum albumin (BSA) and the fluorescein-labeled biotin were purchased from Sigma (St. Louis, MO). Fluorescein-labeled avidin and sulfosuccinimidyl-6-(biotinamido)hexanoate (NHS-LC-biotin) were obtained from Pierce (Oud Beijerland, The Netherlands). (3-Aminopropyl)triethoxysilane (APTS) and mercaptomethyldimethylethoxysilane (MDS) were purchased from Petrarch (Bristol, PA). Chloroform, ethylenediaminetetraacetic acid (EDTA), methanol, nitric acid (65%), poly(acrylic acid) 5100 sodium salt, sodium azide, disodium hydrogen phosphate, toluene, Tween 20, and urea were obtained from Merck (Zürich, Switzerland) or Fluka (Buchs, Switzerland) and were all of analytical grade. The phosphate buffer (pH 7, containing 0.04 M $Na_2HPO_4$ and 0.03 M $KH_2PO_4$) and the deionized water (purified by a filter system from Millipore) were obtained from internal sources.

**Instrumentation.** The instrumental setup of the fiber optic evanescent wave sensor was previously described by Glass et al.[26] and combined with an automated fluid handling system.[27] An argon ion laser (Spectra-Physics, Model 161 C), emitting at 488 nm, was used as an excitation light source, matching the optimal excitation wavelength of fluorescein. The emission light was detected by a photomultiplier (Hamamatsu, Model HC 120−05). The quartz fiber was mounted in a temperature-controlled flow-through cell (built in-house) with a cell volume of 70 μL. Two water baths with different temperatures (switchable by a six-port valve) were applied to change in a short time between the hybridization temperature and the temperature for thermal regeneration. The water bath temperature was adjusted in steps of 5 °C and measured in separate experiments in the flow-through cell at an adequate flow rate using an electric thermometer (Testoterm, Model testo901). The fiber optic sensor was exposed to a flow stream (typical flow rates, 0.5−2 mL/min) using four piston pumps (Metrohm, Model 665). The four piston pumps were used to dispense the hybridization buffer, the tracer, the sample, and the regeneration solution. A 75 μL dynamic mixing chamber (Portmann Instruments), between the flow-through cell and the piston pumps, was used to mix the flow streams before applying them to the sensor. The instrumental setup was controlled by a software program that allowed it to run fully automated assay cycles and data collection. The software program was written in-house and named FOBIA, as an acronym for *f*iber *o*ptic *b*iospecific *i*nteraction *a*nalysis.

**Preparation of the DNA Sensor.** Polished quartz fibers with a length of 65 mm and a diameter of 1 mm were obtained from Ensign-Bickford Optics (Avon, CT) and cleaned by sonicating in 65% $HNO_3$ for 30 min, followed by washing steps in deionized water until pH neutrality. The silica surface was silanized either with APTS (aminosilanized fibers) or MDS (thiolsilanized fibers). For the preparation of aminosilanized fibers, freshly cleaned fibers were immersed for 15 min in a stirred solution consisting of 300 mL of toluene, 30 μL of Tween 20, 300 μL of deionized water, and 300 μL of APTS, followed by rinsing in deionized water. Thiolsilanized fibers were prepared by gas phase silanization for 2 days at 180 °C and 10 mbar using 1 mL of MDS. The quartz fibers were biotinylated either by coupling NHS-LC-biotin[28] covalently to aminosilanized fibers or by binding biotinylated BSA hydrophobically to thiolsilanized fibers. For the biotinylation, silanized fibers were immersed in 0.1 mg/mL NHS-LC-biotin in 0.1 M bicarbonate buffer (pH 8.5) for 3 h at room temperature or in 1 mg/mL biotinylated BSA in 70 mM phosphate buffer (pH 7) overnight at 4 °C, respectively. Then, avidin or streptavidin was bound to the fiber surface by incubating the biotinylated fibers overnight at 4 °C in 70 μL of a solution containing 2.5 mg/mL (strept)avidin and 40 mg/mL Tween 20 in 70 mM phosphate buffer (pH 7). Biotinylated capture probes were bound to


(20) Oroszlan, P.; Duveneck, G. L.; Ehrat, M.; Widmer, H. M. *Sens. Actuators B* **1993**, *11*, 301−305.
(21) *Nonisotopic DNA probe techniques*; Kricka, L. J., Ed.; Academic Press: San Diego, 1992.
(22) *Nonradioactive labeling and detection of biomolecules;* Kessler, C., Ed.; Springer: Berlin, 1992.
(23) Stanley, P. E. *Biolumin. Chemilumin.* **1993**, *8*, 51−63.
(24) *Nucleic acid hybridisation−a practical approach*; Hames, B. D.; Higgins, S. J., Eds.; IRL Press: Oxford, U.K., 1985.
(25) Oroszlan, P.; Thommen, C.; Wehrli, M.; Duveneck, G.; Ehrat, M. *Anal. Methods Instrum.* **1993**, *1*, 43−51.
(26) Glass, T. R.; Lackie, S.; Hirschfeld, T. *Appl. Opt.* **1987**, *26*, 2181−2187.
(27) Oroszlan, P.; Duveneck, G. L.; Ehrat, M.; Widmer, H. M. In *Chemical, Biochemical, and Environmental Fiber Sensors V*, Lieberman, R. A., Ed.; SPIE Proceedings Series 2068; SPIE: Bellingham, WA, 1994; pp 159−167.
(28) Diamandis, E. P.; Christopoulos, T. K. *Clin. Chem.* **1991**, *37*, 625−636.

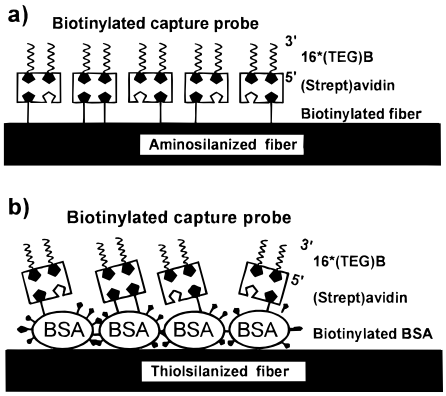


Figure 1. Schematic diagrams of the possible arrangement of immobilized capture probes. (a) The aminosilanized fiber surface was biotinylated with NHS-LC-biotin, and (b) biotinylated BSA was bound hydrophobically to a thiolsilanized quartz fiber. (Strept)avidin and biotinylated oligonucleotides were bound to the surface in two consecutive incubation steps.

Table 1. Oligonucleotides[a]

| designation | sequence |
|---|---|
| | Immobilized Oligonucleotides |
| 16*B | biotin-5′-CACAATTCCACACAAC-3′ |
| 16*BFl | biotin-5′-CACAATTCCACACAAC-3′-fluorescein |
| 16*TEGB | biotin-TEG-5′-CACAATTCCACACAAC-3′ |
| | Complementary Oligonucleotides |
| 16*CFl | fluorescein-5′-GTTGTGTGGAATTGTG-3′ |
| 16*C | 5′-GTTGTGTGGAATTGTG-3′ |
| | Noncomplementary Oligonucleotide |
| 20*Fl | fluorescein-5′-CTGCAACACCTGACAAACCT-3′ |

[a] For definitions, see Abbreviations.

immobilized (strept)avidin by incubating freshly prepared fibers overnight at 4 °C in 70 $\mu$L of a solution containing 100 $\mu$g/mL 16*B or 16*TEGB (Table 1) in 70 mM phosphate buffer (pH 7), resulting in fiber surfaces as illustrated schematically in Figure 1. Before performing an assay, the optical fibers with immobilized oligonucleotides were rinsed in deionized water, blown dry with a stream of nitrogen and inserted into the flow-through cell.

**Hybridization of Immobilized DNA.** Table 1 shows the model systems which were used for the hybridization assays.[29] The immobilized capture probe 16*B or 16*TEGB was hybridized with the complementary strands 16*CFl (tracer DNA) and 16*C (target DNA). In order to determine the amount of nonspecific binding, a noncomplementary, fluorescein-labeled 20-mer oligonucleotide 20*Fl was used.

The DNA hybridization assays were performed in four steps, as illustrated in Figure 2: (1) equilibration of the fiber surface (pH, temperature, etc.), (2) hybridization, (3) washing, and (4) regeneration.

As a hybridization buffer, a solution containing the components shown in Table 2 was used. Poly(acrylic acid) 5100 sodium salt and Tween 20 were used to prevent nonspecific binding caused by ionic or hydrophobic interaction.

## RESULTS AND DISCUSSION

**Thermal and Chemical Regeneration.** Initial DNA hybridization assays were measured using assay cycles with a duration

(29) Graham, C. R.; Leslie, D.; Squirrell, D. J. *Biosens. Bioelectron.* **1992**, *7*, 487–493.

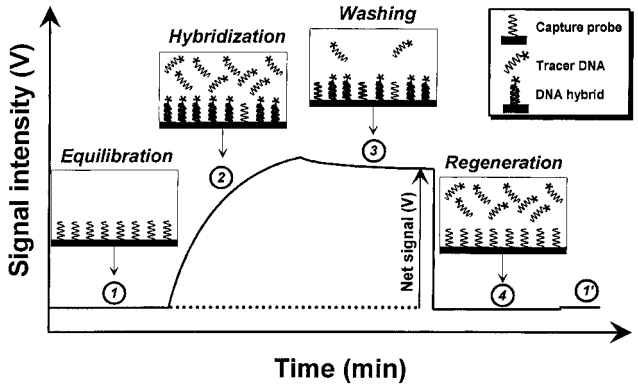


Figure 2. Idealized signal development during the different steps of a hybridization assay cycle.

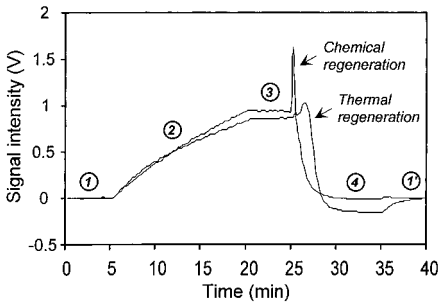


Figure 3. Two assay cycles, in which the regeneration was performed by either thermal or chemical regeneration. The capture probe 16*B was immobilized via NHS-LC-biotin and streptavidin.

Table 2. Preparation of the Hybridization Buffer (pH 7.7)

| | |
|---|---|
| 75 mL | 70 mM phosphate buffer (pH 7, containing 0.04 M $Na_2HPO_4$ and 0.03 M $KH_2PO_4$) |
| 6.5 g | KCl |
| 0.02 g | EDTA·2 $H_2O$ |
| 0.25 g | $NaN_3$ |
| 0.5 g | Poly(acrylic acid) 5100 sodium salt |
| 0.5 g | Tween 20 |
| | adjust to pH 7.7 with 1 M NaOH |
| | fill to 1 L with deionized water |

of 35 min (5 min equilibration, 15 min hybridization, 5 min washing, and 10 min regeneration). During the equilibration and washing steps, the hybridization buffer was pumped through the sample cell at a flow rate of 0.5 mL/min. The hybridization was performed by using a 10 nM 16*CFl solution at a flow rate of 0.5 mL/min.

The regeneration was achieved by either thermal or chemical regeneration (Figure 3). Whereas the temperature was adjusted to 26.7 °C for the hybridization, the fiber surface was heated to a temperature of 68.5 °C for the thermal regeneration ($T_m$ = 54.5 °C). The chemical regeneration was performed at the hybridization temperature, by pumping a 50% (w/w) aqueous urea solution at a flow rate of 0.5 mL/min through the sample cell. After the regeneration, a new assay cycle was started with a 5 min equilibration step.

The four assay steps are accompanied by clearly distinguishable, characterized segments of the signal development (Figure 3). The assay cycle starts with a very stable baseline during the equilibration step. This baseline was always used to put the offset of the measured binding curves to zero. The binding of the fluorescein-labeled complementary strand 16*CFl to the im-

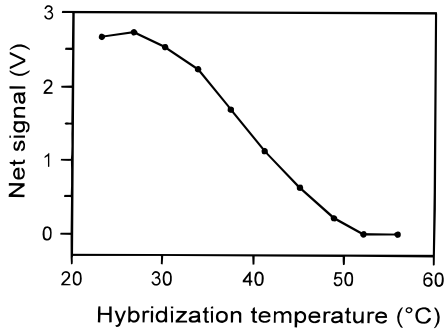


Figure 4. Net fluorescence signal of 10 hybridization assays, which were measured at different hybridization temperatures between 23 and 56 °C, by applying assay cycles of 33 min duration (3 min equilibration, 15 min hybridization with 10 nM 16*CFl, 10 min washing, and 5 min chemical regeneration), at a flow rate of 0.5 mL/min. The net fluorescence signal was determined at the 21st min of an assay cycle. The capture probe 16*B was immobilized via NHS-LC-biotin and avidin.

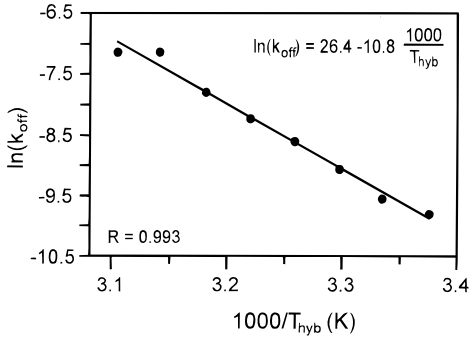


Figure 5. Arrhenius plot of dissociation rates ($k_{off}$) as a function of the hybridization temperature ($T_{hyb}$). The dissociation rates were determined from the signal development during the washing step of hybridization assays, which were measured at different hybridization temperatures between 23 and 49 °C (Figure 4).

mobilized capture probe 16*B could be observed in real time by the increasing fluorescence signal during the hybridization step. The dissociation, observed as a slight decrease of the fluorescence signal during the washing step, was very slow, indicating a high stability of the formed DNA hybrids. The *chemical* regeneration results in a much faster dissociation of the DNA hybrids into single strands and in a more stable baseline compared to the *thermal* regeneration. The reproducibility of the net signal of 35 consecutive assay cycles (using the experimental conditions described above) was also improved by using the chemical instead of the thermal regeneration (results not shown).

At the beginning of the chemical regeneration, a short signal peak can be observed, caused by the change in the refractive index of the hybridization buffer (=1.34) and the 50% urea solution (=1.41). Using a refractive index of 1.00 for air and 1.46 for the quartz fiber, the critical external incident angle can be calculated as 36.1° for the hybridization buffer and 21.9° for the 50% urea solution. The laser beam can only be guided through the optical fiber by total internal reflection when the applied incident angle is smaller than the critical incident angle. In the experiments done in this work, an external incident angle of 33.5° was applied. Consequently, the laser beam is only guided through the fiber while the fiber is surrounded by the hybridization buffer. As long as both the hybridization buffer and the regeneration solution are in the sample cell, light scattering occurs causing the signal peak at the beginning of the regeneration step.

**Hybridization Temperature.** The effect of different hybridization temperatures (between 23 and 56 °C) on the hybridization ability was tested, by applying assay cycles of 33 min duration (3 min equilibration, 15 min hybridization with 10 nM 16*CFl, 10 min washing, and 5 min chemical regeneration). The net fluorescence signals were determined at the 21st min of an assay cycle and are illustrated in Figure 4. At all hybridization temperatures, the regeneration was performed by using a 50% (w/w) aqueous urea solution. The formation of DNA double strands could be observed by using hybridization temperatures up to 49 °C. If a hybridization temperature of 52 °C or higher was used, the DNA sensor surface was damaged irreversibly. The loss in activity is caused most likely by denaturation of the avidin used for immobilization.

During the washing step, the dissociation of the formed DNA hybrids into single strands could be observed as a function of the hybridization temperature. The corresponding dissociation rates ($k_{off}$) were fitted by using a single-exponential eq 1 and were

$$I(t) = Ae^{-k_{off}t} \quad (1)$$

in the range of $5.5 \times 10^{-5}\ s^{-1} \le k_{off} \le 7.9 \times 10^{-4}\ s^{-1}$ for 23 °C < $T_{hyb}$ < 49 °C. The relatively slow dissociation rates at higher temperatures indicate a high stability of the formed double stands.

More information about the dissociation process was obtained by plotting the fitted dissociation rates as a function of the measured hybridization temperatures ($T_{hyb}$). The resulting Arrhenius plot (Figure 5) showed Arrhenius-type behavior in a temperature range of 23 °C < $T_{hyb}$ < 49 °C. From the slope, an activation energy of $E_a$ = 89.5 kJ/mol was determined for the dissociation of the double-stranded DNA hybrids into single strands. This activation energy is too small for the simultaneous separation of the 16 base paired duplex. Therefore, the number of base pairs involved in the strand separation might be 2−3, assuming that the activation energy of the individual base pair separation is about 40 kJ/mol and the melting of several base pairs is the rate-limiting step of the overall dissociation process, as proposed by Ikuta et al.[30,31]

**Short Assay Cycles and Nonspecific Binding.** The coupling of the biotinylated capture probe with the 5′-end to immobilized avidin or streptavidin allows the formation of stable DNA hybrids on the fiber surface, as demonstrated above. Combined with the chemical regeneration the duration of an assay cycle could be reduced to 3 min, as illustrated in Figure 6. In order to increase the selectivity of hybridization,[32] a hybridization temperature of 32.9 °C was chosen. By using flow rates of 2 mL/min and a 10 nM 16*CFl solution for the hybridization, a net signal of more than 1300 mV was observed. The baseline was very stable, with a signal variation of ±8.6 mV. The amount of nonspecific binding, measured with a noncomplementary fluorescein-labeled 20-mer oligonucleotide 20*Fl, was 1.3%, compared with the specific binding signal.

**Four Hundred Consecutive Assay Cycles.** Four hundred consecutive assay cycles were measured, in order to study the

(30) Ikuta, S.; Takagi, K.; Wallace, R. B.; Itakura, K. *Nucleic Acids Res.* **1987**, *15*, 797−811.
(31) Patel, D. J., Ikuta, S.; Kozlowski, S.; Itakura, K. *Proc. Natl. Acad. Sci. U.S.A.* **1983**, *80*, 2184−2188.
(32) Wallace, R. B.; Shaffer, J.; Murphy, R. F.; Bonner, J.; Hirose, T.; Itakura, K. *Nucleic Acids Res.* **1979**, *6*, 3543−3557.

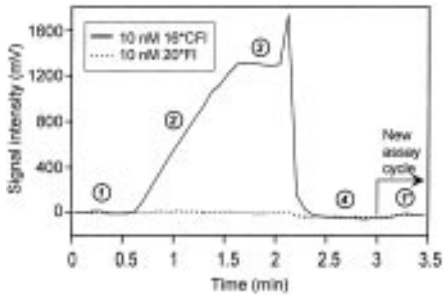


Figure 6. Two assay cycles with a duration of 3 min per cycle. The dotted line shows the amount of nonspecific binding of a fluorescein-labeled noncomplementary oligonucleotide 20*Fl. The capture probe 16*B was immobilized via NHS-LC-biotin and avidin.

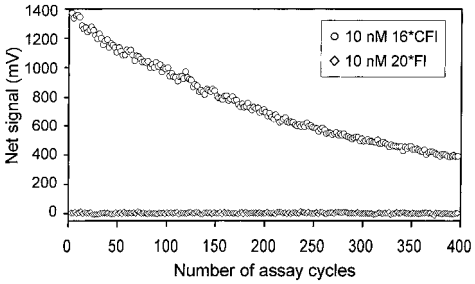


Figure 7. Four hundred consecutive assay cycles. The hybridization assays were performed by following the same assay protocol as used for the experiment illustrated in Figure 6, whereas the incubation with the complementary and noncomplementary oligonucleotide was alternated. The capture probe 16*B was immobilized via NHS-LC-biotin and avidin.

stability of the DNA sensor, the reproducibility of the measured net signal, and the amount of nonspecific binding over an extended period of sensor use (Figure 7). The hybridization assays were performed using the same experimental conditions as applied for the experiments illustrated in Figure 6, whereas the incubation with the complementary 16*CFl and the noncomplementary oligonucleotide 20*Fl was alternated. The sensor response resulted in a net signal with a nearly single-exponential signal loss. The gradual signal loss in consecutive assay cycles can be described by the decay constant $k_{fit}(32.9\ °C) = (1.44 \pm 0.01 \times 10^{-5}\ s^{-1}$, corresponding to a signal loss of 0.16% per assay cycle and a reduction of the initial net signal to 50% after 218 cycles. The measured net signals $I(t)_{exp}$ can be corrected to $I(t)_{corr}$ by using eq 2.

$$I(t)_{corr} = I(t)_{exp} / e^{-k_{fit}t} \qquad (2)$$

The corrected net signals could be fitted by a straight line with a relative standard deviation of 2.4%. The amount of nonspecific binding during the 400 consecutive assay cycles was between 1 and 2%.

**Sensor Stability.** For all the hybridization experiments described so far, the biotinylated capture probe 16*B was immobilized using aminosilanized fibers, NHS-LC-biotin, and avidin or streptavidin. With respect to stability, reproducibility, signal intensities, and nonspecific binding, no significant differences were found between utilizing avidin or streptavidin for the immobilization of the capture probe.

In a next step, 16*B was immobilized using thiolsilanized fibers, biotinylated BSA, and avidin. The stability of the immobilization of the capture probe was tested, using assay cycles with a duration of 38 min (5 min equilibration, 15 min hybridization, 15 min washing, and 3 min regeneration), for all the systems illustrated in Figure 8. During the hybridization step, the hybridization buffer was used for systems 1−3, and a 10 nM 16*CFl solution was used for systems 4 and 5; the flow rate was always 0.5 mL/min. Systems 1−4 represent the different steps used for the immobilization of a biotinylated capture probe via biotinylated BSA and avidin. System 5 was used to compare the stability of covalent and hydrophobic immobilization of biotin on silanized fibers.

Only the net signals from the last 38 cycles (24 h) of the 50 measured assay cycles are illustrated in Figure 9 and were used to calculate the signal loss, by applying a single-exponential fit. The resulting values for the signal loss $k_1-k_5$ are shown in Table 3.

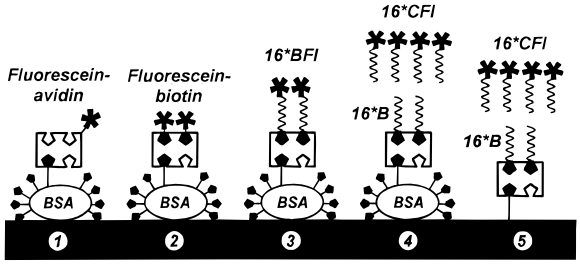


Figure 8. Model systems used to investigate the cause of the signal loss during long-time measurements such as consecutive assay cycles. Avidin was used for all immobilizations.

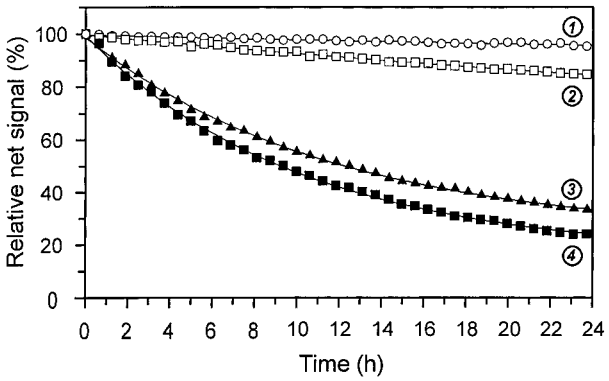


Figure 9. Relative net signals during 24 h for assay cycles of 38 min duration (5 min equilibration, 15 min hybridization, 15 min washing, and 3 min chemical regeneration) performed with systems 1−4 (Figure 8), using a hybridization temperature of 33.7 °C at a flow rate of 0.5 mL/min. During the hybridization step, the hybridization buffer (systems 1−3) or a 10 nM 16*CFl solution (system 4) was applied.

Table 3. Calculated Values ($k_1-k_5$) of the Signal Loss from the Curves Illustrated in Figure 8[a]

$k_{1,\ \text{fluorescein-avidin}} = (4.84 \pm 0.20) \times 10^{-7}\ s^{-1}$
$k_{2,\ \text{fluorescein-biotin}} = (2.01 \pm 0.03) \times 10^{-6}\ s^{-1}$
$k_{3,\ 16*\text{BFl}} = (2.33 \pm 0.03) \times 10^{-5}\ s^{-1}$
$k_{4,\ 16*\text{B}} = (2.54 \pm 0.05) \times 10^{-5}\ s^{-1}$
$k_{4,\ 16*\text{TEGB}} = (1.03 \pm 0.05) \times 10^{-5}\ s^{-1}$
$k_{5,\ 16*\text{B}} = (2.68 \pm 0.06) \times 10^{-5}\ s^{-1}$
$k_{\text{off, avidin-biotin}}\ (25\ °C) = 6.3 \times 10^{-8}\ s^{-1}$
$k_{\text{off, avidin-LC-biotin}}\ (25\ °C) = 1.1 \times 10^{-7}\ s^{-1}$

[a] $k_{4,\ 16*\text{TEGB}}$ is corresponding to system 4 by using 16*TEGB instead of 16*B as a capture probe. The hybridization temperature was 33.7 °C.

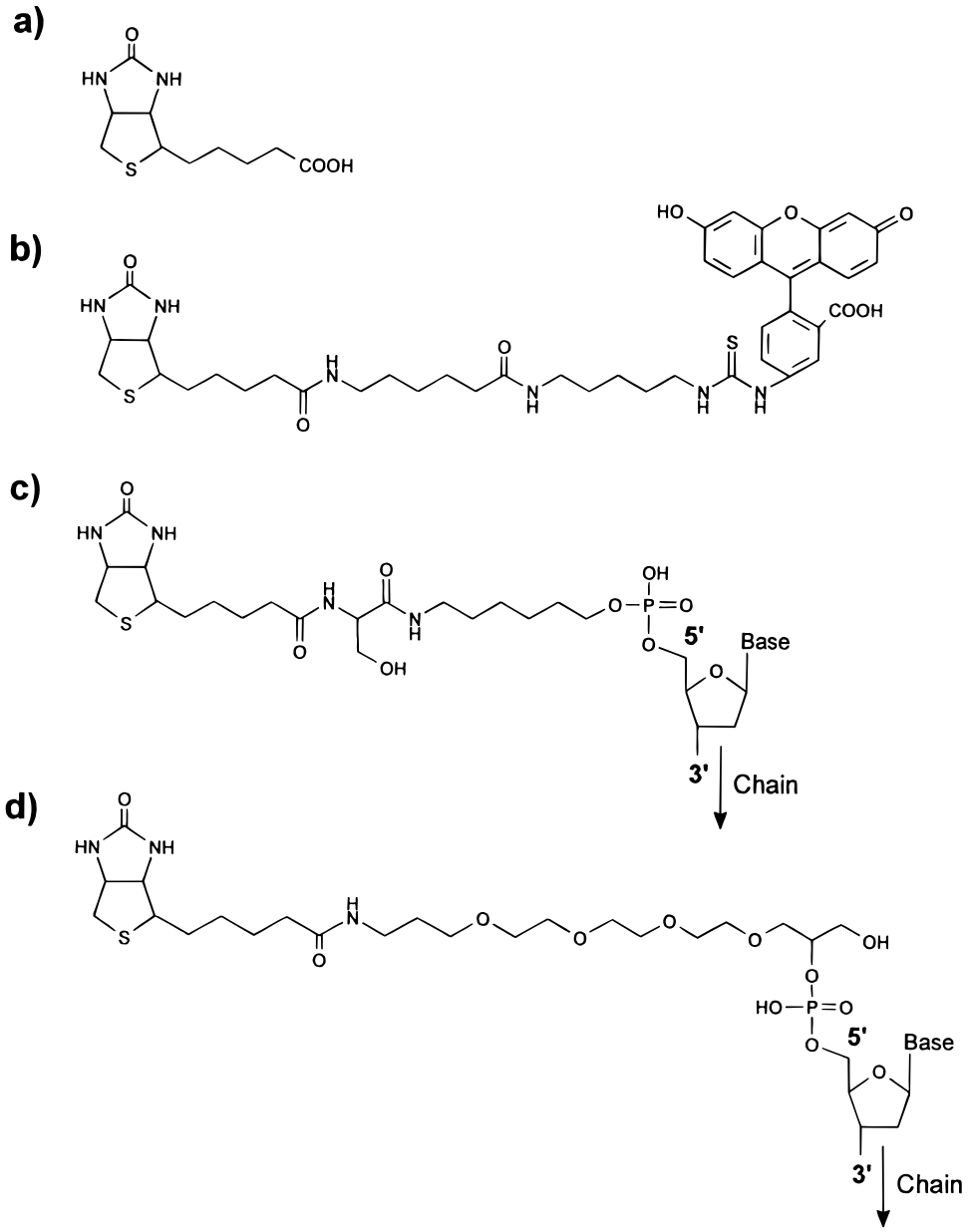


Figure 10. (a) Structure of native biotin, also known as vitamin H. (b) Fluorescein-labeled biotin derivative, which was used for measuring the dissociation kinetics of biotin bound to the fiber surface via avidin. (c) Structure of the biotinylated capture probe 16*B. (d) Structure of the biotinylated capture probe 16*TEGB with a triethylene glycol spacer between the capture probe and the biotin.

The values of $k_1$ and $k_2$ represent the dissociation rates of the avidin−biotin affinity system at a temperature of 33.7 °C and are of an order of magnitude similar to values given in the literature. The affinity constant of the avidin−biotin system is $K = 10^{15}$ M$^{-1}$, whereas the dissociation rate is given as $k_{off} = 6.3 \times 10^{-8}$ s$^{-1}$ for native biotin[33] (Figure 10a) and $k_{off} = 1.1 \times 10^{-7}$ s$^{-1}$ for a biotin derivative with a spacer arm as illustrated in Figure 10b,[33] at a temperature of 25 °C.

The values of $k_3$−$k_5$ were much higher than the dissociation rate of the avidin−biotin system. The influence of the regeneration time on the signal loss was tested by applying a 50% (w/w) aqueous urea solution for 10 instead of 3 min. The resulting values of $k_3$−$k_5$ were not affected by using a longer regeneration time, which indicates that the signal loss is not caused by the regeneration step. If denaturation of the proteins BSA or avidin, resulting in inaccessibility of the capture probe for complementary strands, would be responsible for the signal loss, $k_3$ should be much slower than $k_4$ and $k_5$. A digestion of the nucleic acids by nucleases is also unlikely, because of the reproducibility of the signal loss and the absence of any indication for enzymatic degradation of immobilized oligonucleotides, when other immobilization methods were applied. The structure of the biotinylated capture probe 16*B is shown in Figure 10c. By comparing the structure of the spacer arm of this derivative with the spacer arm of the fluorescein-labeled biotin (Figure 10b) or with the structure of native biotin (Figure 10a), we hypothesized that the structural difference could be the reason for a higher dissociation rate of the biotin derivatives used in the systems 3−5 (16*B and 16*BFl).

In order to improve the sensor stability, 16*TEGB as another capture probe with a triethylene glycol (TEG) spacer arm between

(33) Finn, F. M.; Hofmann, K. H. *Methods Enzymol.* **1985**, *109*, 418−445.

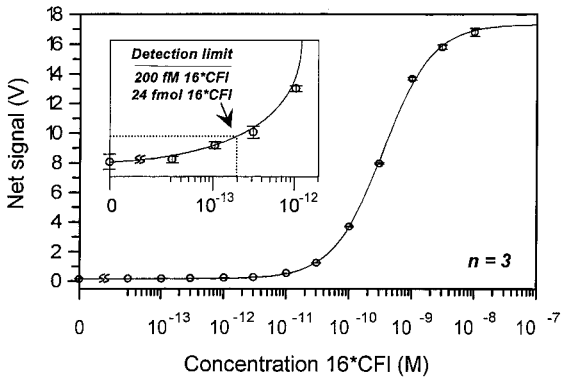


Figure 11. Dose−response curve of the hybridization with the tracer DNA 16*CFl. The error bars correspond to the standard deviation of three measurements ($n$ = 3). The hybridization assays were performed at 32.9 °C: 10 min equilibration, 60 min hybridization (0−10 nM 16*CFl), 5 min washing, and 5 min chemical regeneration. The capture probe 16*TEGB was immobilized via biotinylated BSA and avidin.

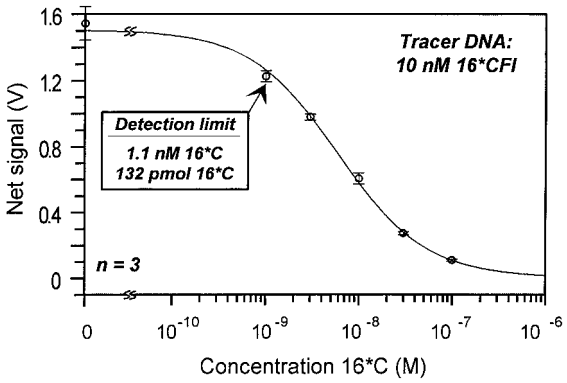


Figure 12. Dose−response curve of the competitive hybridization assay with the target DNA 16*C, using a constant tracer DNA concentration of 10 nM 16*CFl. The error bars correspond to the standard deviation of three measurements ($n$ = 3). The hybridization assays were performed at 32.9 °C, at a flow rate of 2 mL/min: 10 min equilibration, 60 min hybridization (0−100 nM 16*C), 5 min washing, and 5 min chemical regeneration. The capture probe 16*TEGB was immobilized via biotinylated BSA and avidin.

the biotin and the oligonucleotide (Figure 10d) was tested. Although the signal loss could be reduced to $k_{16*TEGB} = 1.0 \times 10^{-5}$ s$^{-1}$, this value is still 5 times larger than the dissociation rate $k_2$ of the fluorescein-labeled biotin.

**Dose−Response Curves for Hybridization Assays.** Figures 11 and 12 show two dose−response curves of hybridization assays, in which the capture probe 16*TEGB was immobilized using thiolsilanized fibers, biotinylated BSA, and avidin. In order to obtain a calibration curve for the detection of the tracer DNA 16*CFl, hybridization assays were performed using different concentrations of the tracer DNA (0−10 nM 16*CFl) and an incubation time of 60 min, at a flow rate of 2 mL/min. Averages of the resulting net signals from three measurements, after correction for the signal loss, together with the corresponding standard deviations, are plotted as a function of the logarithmic value of the tracer DNA concentration (Figure 11).

The average standard deviation of all measurements was 1.3%. The detection limit was determined by adding three standard deviations of the measurement in absence of the tracer DNA (0 nM 16*CFl) to the corresponding average net signal, assigning the resulting signal value to the concentration using the dose−response curve. The detection limit for the hybridization with the complementary fluorescein-labeled oligonucleotide was determined as $2.0 \times 10^{-13}$ M, corresponding to 24 fmol or 1.3 pg/mL 16*CFl. Based on this dose−response curve, an assay working range of nearly five decades ($10^{-13}$−$10^{-8}$ M) can be achieved.

With a new fiber, using 16*TEGB as a capture probe, a dose−response curve was generated for the detection of the complementary unlabeled target DNA 16*C. In competitive hybridization assays the target DNA was incubated for 60 min at concentrations between 0 and 100 nM 16*C, whereas each concentration was measured three times. The tracer DNA was incubated simultaneously with the target DNA by using a constant tracer DNA concentration of 10 nM 16*CFl.

After correction for the signal loss, the resulting average net signals, together with the corresponding standard deviations, are plotted as a function of the logarithmic value of the target DNA concentration (Figure 12).

The detection limit for the competitive hybridization with the complementary unlabeled oligonucleotide was determined to be $1.1 \times 10^{-9}$ M, which corresponds to 132 pmol or 660 pg/mL 16*C. The working range for the competitive hybridization assay covered two decades ($10^{-9}$−$10^{-7}$ M). The average standard deviation of all measurements was 4.2%. For improved sensitivity of the competitive hybridization, the amount of binding sites on the sensor surface would have to be reduced and the tracer DNA concentration would have to be optimized.

## CONCLUSIONS

Biotinylated capture probes could be immobilized on optical fibers using the (strept)avidin−biotin affinity system. Hybridization with a complementary DNA strand resulted in stable double helices, which could be dissociated efficiently with a 50% urea solution for chemical regeneration of the sensor surface. This allowed us to perform short assay cycles, with a duration of 3 min or even less, and to perform hundreds of consecutive assay cycles with the same fiber. The chemical regeneration of the sensor surface was so efficient that the background signal did not significantly increase, even after hundreds of assay cycles. The signal loss during consecutive assay cycles was nearly single exponential, which simplifies the application of a signal correction. Additionally, the signal loss was independent of the concentration of tracer DNA and target DNA employed, allowing measurment of different analyte concentrations, which can all be corrected for the signal loss by the same correction function. No significant differences in the sensor stability and the sensor performance were found by immobilizing the biotin either covalently or hydrophobically on the sensor surface or by using avidin or streptavidin for the immobilization of the biotinylated capture probe.

The automated fluid and data handling system, combined with the multiuse DNA sensor, permits analysis of a high number of samples, with a high reproducibility and the possibility of monitoring the binding events directly during the measurement. By applying longer assay cycles, with an incubation time of 60 min, a fluorescein-labeled complementary 16-mer oligonucleotide could be detected to a concentration of $2.0 \times 10^{-13}$ M (24 fmol), with an assay working range spanning almost five decades ($10^{-13}$−$10^{-8}$ M). Competitive hybridization assays were performed for the detection of unlabeled complementary 16-mer oligonucleotide, by applying a 10 nM tracer DNA concentration, resulting in a detection limit of $1.1 \times 10^{-9}$ M (132 pmol).

Nevertheless, the achieved sensitivity is not yet sufficient for all applications, and further efforts have to be made to improve the sensitivity and stability of the DNA sensor. A hybridization assay, e.g., for the direct detection of a specific genomic sequence of an infectious disease, would need a sensitivity allowing detection of $10^4-10^5$ copies of a specific target DNA.[34] With the sensitivity achieved, it was possible to detect about $10^{10}$ oligonucleotides; i.e., the sensitivity of the DNA sensor is not yet sufficient for in vitro diagnostic tests. There are some possibilities to increase the sensitivity of the DNA sensor further, e.g., by decreasing the used sample volume during the hybridization step or by applying an amplification system, such as multilabeling. In addition, an amplification system prior to the detection could be applied, such as the polymerase chain reaction (PCR).[35−37] PCR also allows labeling of DNA with fluorescein or another marker during amplification.[38]

The amount of nonspecific binding, tested by application of a noncomplementary oligonucleotide was very low; poly(acrylic acid) 5100 sodium salt and Tween 20 were used in the hybridization buffer to prevent nonspecific binding caused by ionic or hydrophobic interaction.

**Abbreviations:** 16*, 16-mer oligonucleotide; APTS, (3-aminopropyl)triethoxysilane; B, biotin; BSA, bovine serum albumin; C, complementary DNA strand; EDTA, ethylenediaminetetraacetic acid; Fl, fluorescein; FOBIA, fiber-optic biospecific interaction analysis; LC, long chain; MDS, mercaptomethyldimethylethoxysilane; NHS, *N*-hydroxysuccinimide; PAGE, polyacrylamide gel electrophoresis; PCR, polymerase chain reaction; TEG, triethylene glycol; $T_m$, melting temperature.


## ACKNOWLEDGMENT

The authors are thankful to Drs. Dieter Hüsken, Uwe Pieles, and Heinz Moser for helpful discussions.

Received for review January 24, 1996. Accepted May 31, 1996.[⊗]

AC960071+



(34) Diamandis, E. P. *Clin. Chim. Acta* **1990**, *194*, 19−50.
(35) Veringa, E. M.; Zuyderwijk, M. A. M.; Schellekens, H. *J. Microbiol. Methods* **1994**, *19*, 117−125.
(36) Luk, J. M. C. *BioTechniques* **1994**, *17*, 1038−1042.
(37) Gibellini, D.; Zauli, G.; Re, M. C.; Furlini, G.; Lolli, S.; Bassini, A.; Celeghini, C.; La Placa, M. *Anal. Biochem.* **1995**, *228*, 252−258.
(38) Remick, D. G.; Kunkel, S. L.; Holbrook, E. A.; Hanson, C. A. *Am. J. Clin. Pathol.* **1990**, *93* (Suppl 1), S49−S54.



[⊗] Abstract published in *Advance ACS Abstracts,* July 15, 1996.